

AD-A071 856

AERONAUTICAL RESEARCH ASSOCIATES OF PRINCETON INC NJ

F/G 20/4

PRELIMINARY STUDY BY MEANS OF SECOND-ORDER CLOSURE OF THE HEAT --ETC(U)

JAN 78 C D DONALDSON, A K VARMA

N60921-77-C-0242

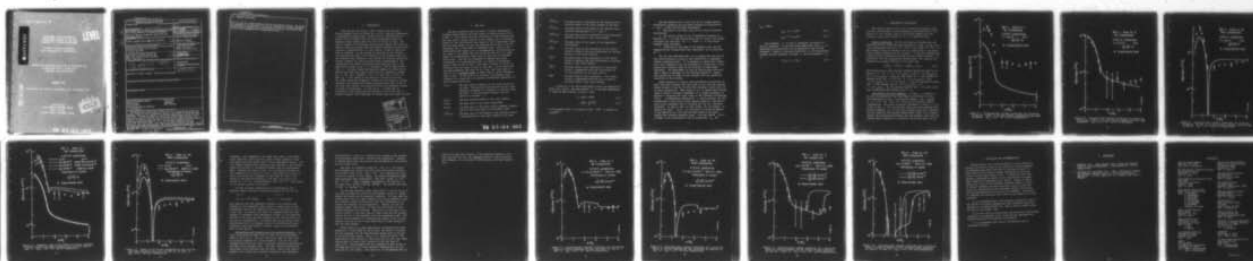
NL

UNCLASSIFIED

ARAP-329

| OF |

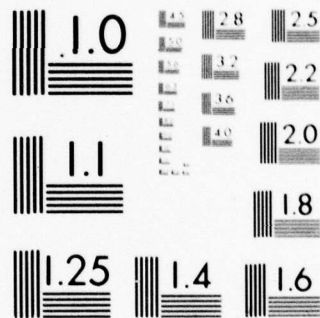
AD  
A071856



END  
DATE  
FILMED

8-79

DDC



MICROCOPY RESOLUTION TEST CHART  
NATIONAL BUREAU OF STANDARDS-1963-A

REPORT NO. 329

PRELIMINARY STUDY BY MEANS OF  
SECOND-ORDER CLOSURE OF THE HEAT  
TRANSFER TO A POROUS SPHERE/CONE

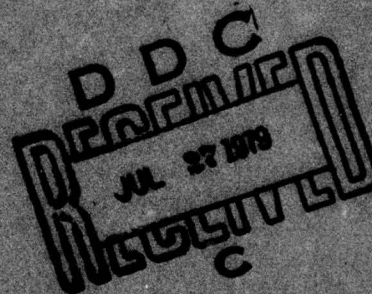
EFFECTS OF SURFACE ROUGHNESS,  
EDGE TURBULENCE AND TRANSPIRATION

NAUTICAL RESEARCH ASSOCIATES OF PRINCETON, INC.  
50 WASHINGTON ROAD, P.O. BOX 2229  
PRINCETON, NEW JERSEY 08540

JANUARY 1978

REPORT FOR PERIOD 30 SEPTEMBER 1977- 30 JANUARY 1978

PREPARED FOR  
NAVAL SURFACE WEAPONS CENTER  
WHITE OAK LAB  
SILVER SPRING, MARYLAND 20910



79 07 24 051

UNCLASSIFIED

SECURITY CLASSIFICATION OF THIS PAGE (When Data Entered)

REPORT DOCUMENTATION PAGE		READ INSTRUCTIONS BEFORE COMPLETING FORM
1. REPORT NUMBER	2. GOVT ACCESSION NO.	3. SPECIFIC CATALOG NUMBER
4. TITLE (and Subtitle) PRELIMINARY STUDY BY MEANS OF SECOND-ORDER CLOSURE OF THE HEAT TRANSFER TO A POROUS SPHERE/CONE. Effects of Surface Roughness, Edge Turbulence and Transpiration,		5. TYPE OF REPORT & PERIOD COVERED Final Report, 30 Sept 1977-30 Jan 1978
7. AUTHOR(s) Coleman duP./Donaldson and Ashok K. Varma		6. PERFORMING ORG. REPORT NUMBER A.R.A.P. Report No. 329 ✓ 8. CONTRACT OR GRANT NUMBER(s) N60921-77-C-0242
9. PERFORMING ORGANIZATION NAME AND ADDRESS Aeronautical Research Associates of Princeton, Inc. 50 Washington Road, P.O. Box 2229 Princeton, NJ 08540		10. PROGRAM ELEMENT, PROJECT, TASK AREA & WORK UNIT NUMBERS 61153N; SF32-322; 18635; SEA 18451-SUM-32
11. CONTROLLING OFFICE NAME AND ADDRESS Naval Surface Weapons Center, WOL White Oak, Silver Spring, MD 20910 Attn: Code WA-43		12. REPORT DATE January 1978
14. MONITORING AGENCY NAME & ADDRESS (if different from Controlling Office) (14) ARAP-329 (12) 27p.		13. NUMBER OF PAGES 24
16. DISTRIBUTION STATEMENT (of this Report) Approved for public release. Distribution unlimited.		15. SECURITY CLASS. (of this report) UNCLASSIFIED
17. DISTRIBUTION STATEMENT (of the abstract entered in Block 20, if different from Report)		15a. DECLASSIFICATION/DOWNGRADING SCHEDULE (16) F32322
18. SUPPLEMENTARY NOTES		
19. KEY WORDS (Continue on reverse side if necessary and identify by block number) Turbulent Boundary Layers      Transition Blunt Bodies      Roughness Conical Bodies      Heat Transfer Second-Order Closure Modeling of Turbulence		
20. ABSTRACT (Continue on reverse side if necessary and identify by block number) A compressible second-order closure code for calculating the behavior of boundary layers on blunt axisymmetric bodies at zero angle of attack has been developed. The code is capable of calculating these boundary layers both with and without rotation and both with and without surface mass injection. Pre- liminary calculations have been made with the code to compare with NSWC measure- ments on a sphere/cone body at $M = 5$ and Reynolds numbers per foot of $3.8 \times 10^6$ and $17.6 \times 10^6$ . The effects of surface roughness and edge turbulence have been investigated. The initial theoretical predictions (cont.)		

DD FORM 1 JAN 73 1473

EDITION OF 1 NOV 65 IS OBSOLETE

UNCLASSIFIED

SECURITY CLASSIFICATION OF THIS PAGE (When Data Entered)



UNCLASSIFIED

SECURITY CLASSIFICATION OF THIS PAGE(When Data Entered)

20. ABSTRACT (concluded)

from the code are in good agreement with the experimental results. The results are dependent on the choices for the surface roughness and the edge turbulence parameters and it appears that a more extensive parametric search could lead to even better agreement with the experimental data.

UNCLASSIFIED

SECURITY CLASSIFICATION OF THIS PAGE(When Data Entered)

## 1. INTRODUCTION

Over the past few months, under funding from the Naval Surface Weapons Center at White Oak, A.R.A.P. has made operational a compressible second-order closure code for computing the behavior of the boundary layer on blunt axisymmetric bodies at supersonic Mach numbers when the angle of attack is zero. The code is capable of calculating such boundary layers both with and without rotation and both with and without continuous surface mass injection (transpiration) of a gas similar to that in which the body is immersed. In the process of checking out the program, calculations were made of the behavior of the boundary layer and the turbulent heat transfer to the surface of a porous sphere/cone without rotation but both with and without transpiration. The configuration for which calculations were made was that of the sphere/cone tested by Mr. R. H. Feldhuhn at NSWC at Mach number 5 (Ref. 1). The Mach number and Reynolds numbers for which calculations were made were those reported in the reference, namely,  $M_\infty = 5$  and  $Re_N = \bar{u}_\infty R_N / \bar{\nu}_\infty = 6.33 \times 10^5$  and  $Re_N = 2.95 \times 10^6$ . Here  $R_N$  is the radius of the spherical portion of the body. For these conditions parametric studies of the effects of surface roughness and boundary-layer-edge turbulence were made to see if the code could predict the reported results for reasonable values of these two parameters. In this way it was hoped that an evaluation of the usefulness and capability of the new code to predict boundary layer phenomena on reentry nose tips might be made.

Accession For	
NTIS GRA&I	<input checked="checked" type="checkbox"/>
DDC TAB	<input type="checkbox"/>
Unannounced	
Justification	
By _____	
Distribution/	
Availability Codes	
Dist	Avail and/or special
<input checked="checked" type="checkbox"/>	

## 2. THE CODE

The basic equations that are used to predict compressible boundary layer behavior on blunt bodies of revolution are given in Ref. 2. Also given there are the details of the modeling that has been used to obtain closure of the original set of equations. Values for the coefficients that appear in this compressible model have not been chosen nor are they adjusted in any way to fit the particular set of data that is considered here. Those of the coefficients that appear also in incompressible flow modeling are set equal to the values that have given the best fit to a large number of incompressible flows, many of which are not boundary layer flows. The rest are evaluated by analogy with their counterparts in incompressible flow, or, where no counterpart exists, they are set to zero. More than a quarter of the 41 coefficients are set equal to zero in this way. In the sense that the same parameters are used for all flows, the full model is said to be an invariant model of shear flows in which turbulence plays a part. In the case of no rotation, the complete model consists of a closed set of 13 partial differential equations for the following quantities:

$\bar{u}(s,n)$	The mean velocity parallel to the local surface of the body. The equations specify this and all other dependent variables as a function of distance along the body $s$ and the normal distance from the surface of the body $n$ .
$\bar{v}(s,n)$	The mean velocity normal to the local surface.
$\bar{T}(s,n)$	The mean value of the local temperature.
$\bar{p}(s,n)$	The mean value of the local static pressure, assumed given at the outer edge of the boundary layer.
$\overline{u'^2}(s,n)$	The mean value of the square of the velocity fluctuations parallel to the local surface of the body.



$\overline{v'^2}(s,n)$	The mean value of the square of the velocity fluctuations normal to the local surface of the body.
$\overline{w'^2}(s,n)$	The mean value of the square of the velocity fluctuations perpendicular to $u'$ and $v'$ .
$\overline{u'v'}(s,n)$	The mean value of the correlation of the velocities parallel and normal to the local surface.
$\overline{T'^2}(s,n)$	The mean value of the square of the temperature fluctuations.
$\overline{\rho'u'}$	The mean value of the correlation of the fluctuations in density with the fluctuations in velocity parallel to the local surface.
$\overline{\rho'v'}$	The mean value of the correlation of the fluctuations in density with the fluctuations in velocity normal to the local surface.
$\overline{T'u'}$	The mean value of the correlation of the fluctuations in temperature with the fluctuations in velocity parallel to the local surface.
$\overline{T'v'}$	The mean value of the correlation of the fluctuations in temperature with the fluctuations in velocity normal to the local surface.

In addition to the above quantities we have the equations of state which relate the mean density  $\bar{\rho}$  to the mean temperature  $\bar{T}$  when the mean pressure is known. Thus

$$\bar{p} = R(\bar{\rho}\bar{T} + \overline{\rho'T'}) \quad (2.1)$$

$$= R\left(\bar{\rho}\bar{T} - \frac{\bar{\rho}}{\bar{T}} \overline{T'^2}\right) \quad (2.2)$$

In the present model, as indicated above,  $\overline{\rho'T'}$  is modeled as  $-(\bar{\rho}/\bar{T})\overline{T'^2}$ .



The code permits one to solve the set of coupled partial differential equations for the above variables as functions of  $s$  and  $n$  given the following information:

1. The shape of the blunt body and its inviscid pressure distribution.
2. The initial values of all 13 dependent variables as a function of  $n$  at some station which may be close to the stagnation point but such that  $s/\delta \gg 1$  where  $\delta$  is the initial boundary layer thickness.
3. Conditions at the edge of the boundary layer and the temperature and transpiration wall conditions, all as functions of  $s$ .

For the runs discussed here, it is assumed that the flow at the initial station is close to the solution for a completely laminar stagnation point. It is possible to remove this restriction, but a program is not yet available for solving for a stagnation point boundary layer in the presence of free-stream turbulence. The development of such an initializing code would seem a logical complement to the existing program if, indeed, this program can be shown to give insights into the problem of transition on blunt bodies.

Before going on to discuss some preliminary calculations of blunt body heat transfer that were made to test the code, mention should be made of the way in which the turbulence scales were set in these calculations. When using A.R.A.P.'s second-order-closure codes to predict turbulent phenomena, it is always necessary to specify or calculate the local scale of the turbulent fluctuations  $\Lambda(s,n)$ . A differential equation for  $\Lambda$  may be written, but the coefficients of the terms in this equation depend on the anisotropy of the turbulence that is produced and are not, therefore, invariant. In view of this, we have chosen, for the present, to specify the scale  $\Lambda(s,n)$  as a function of certain parameters of the mean flow in a way that has been shown to give good results for turbulent boundary layers. For this reason,  $\Lambda(s,n)$  is taken to be the minimum of the two quantities  $\Lambda_{in}$  and

$\Lambda_{out}$  where

$$\Lambda_{in} = \Lambda_o + 0.65n \quad (2.3)$$

$$\Lambda_{out} = 0.17\delta_{.99}(s) \quad (2.4)$$

The parameter  $\Lambda_o$  is used to represent the effects of surface roughness. It has been found empirically that  $\Lambda_o$  is approximately proportional to the magnitude of the surface roughness. Indeed, it has been found that a useful equivalence between surface roughness of height  $k$  and the parameter  $\Lambda_o$  is

$$6.5\Lambda_o < k < 13\Lambda_o \quad (2.5)$$

### 3. PRELIMINARY CALCULATIONS

The first use made of the A.R.A.P. blunt body boundary layer code was, as mentioned in the introduction, the prediction of the behavior of the boundary layer on the porous sphere/cone transpiration cooled model tested at  $M = 5$  at NSWC/White Oak.

Initial conditions. For the calculations reported here the following initial conditions were specified at  $s/R_N = s_1/R_N = 0.1$ . (The corresponding values of  $s/\delta$  were in the range  $30 < s/\delta < 70$ .) The boundary layer was assumed to be of a form close to the appropriate laminar stagnation point solution. It was also assumed that a small velocity disturbance existed in this initial boundary. In particular, for the calculations reported here, the velocity disturbance was assumed isotropic in the sense that

$$(\overline{u'u'})_1 = (\overline{v'v'})_1 = (\overline{w'w'})_1 = q_1^2/3 \quad (3-1)$$

The distribution of this initial turbulent energy was taken to be:  $q_1^2(s_1, n) = 0$  for  $0 < n < 0.12\delta_{.99}(s_1)$ ; from  $n = 0.12\delta_{.99}(s_1)$  to  $n = 0.2\delta_{.99}(s_1)$ ,  $q_1^2(s_1, n)$  was linear in  $n$  and reached its maximum value  $q_1^2 = 3 \times 10^{-5} \bar{u}_\infty^2$  at  $n = 0.2\delta_{.99}(s_1)$ ; from  $n = 0.2\delta_{.99}(s_1)$  to  $n = 0.3\delta_{.99}(s_1)$ ,  $q_1^2(s_1, n)$  decreased linearly with  $n$  and reached zero at  $n = 0.3\delta_{.99}(s_1)$ ; for  $n > 0.3\delta_{.99}(s_1)$ ,  $q_1^2$  was assumed equal to zero. All other turbulent correlations were assumed zero at  $s_1$ .

Calculations for zero roughness. In Figs. 3.1 through 3.4 we show calculations of the heat transfer coefficient for the test sphere/cone of Ref. 1 at Reynolds numbers,  $Re_N = \bar{u}_\infty R_N / \bar{\nu}_\infty$ , of  $6.3 \times 10^5$  and  $2.95 \times 10^6$  both with and without surface transpiration. The cases calculated correspond to cases 1, 2, 22, and 81 of Ref. 1. The calculations shown were made assuming zero surface roughness ( $\Lambda_0 = 0$ ) and zero boundary-layer-edge turbulence. For both high and low Reynolds numbers where there is no transpiration, the calculations indicate that the boundary layer will not undergo early transition to turbulent flow for the small initial



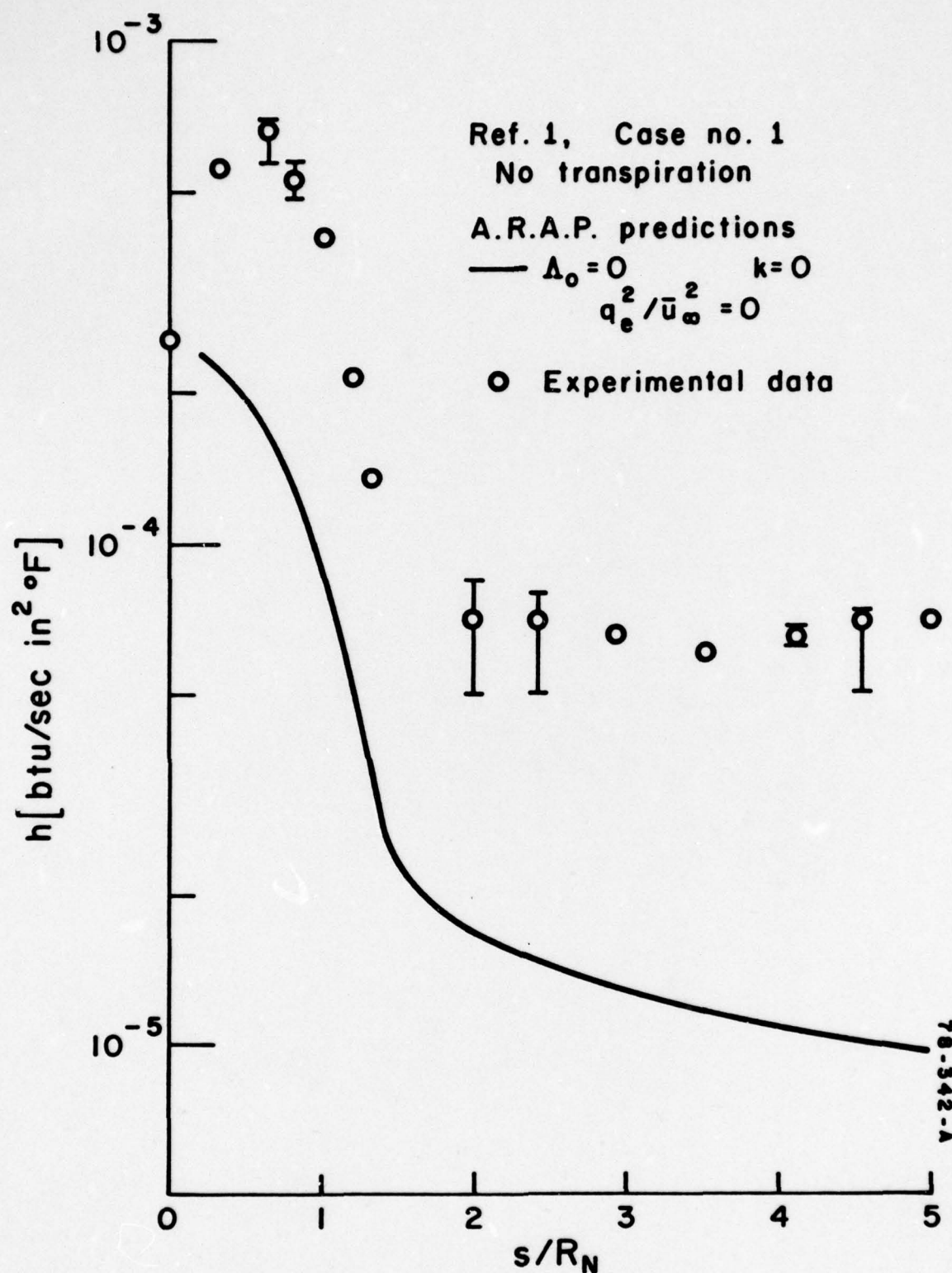


Figure 3.1. Calculated heat transfer coefficient for conditions of Case No. 1 (Ref. 1) for zero surface roughness and zero edge turbulence.  $Re_N = 2.95 \times 10^6$  and no transpiration.



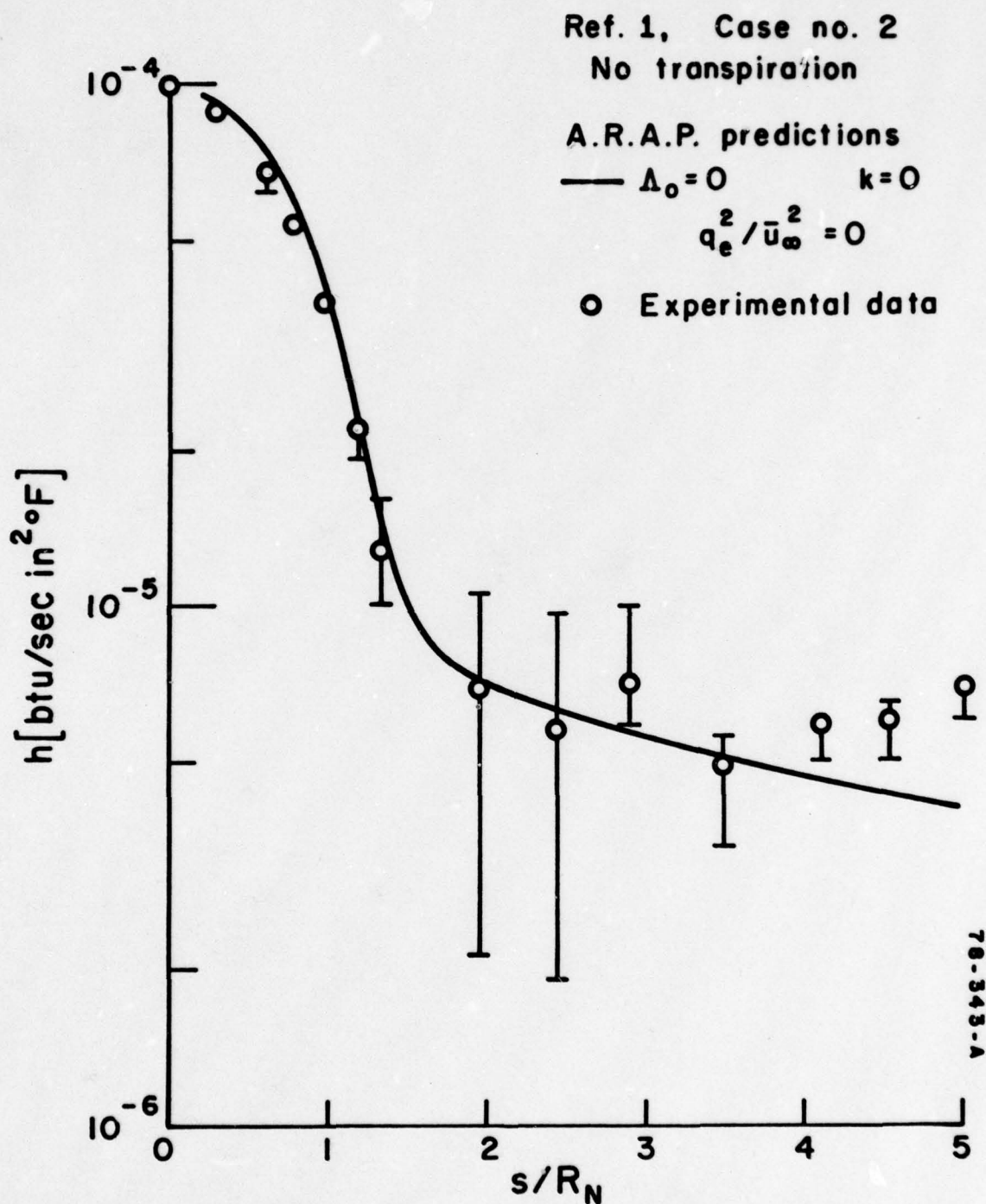


Figure 3.2. Calculated heat transfer coefficient for conditions of Case No. 2 (Ref. 1) for zero surface roughness and zero edge turbulence.  $Re_N = 6.33 \times 10^5$  and no transpiration.

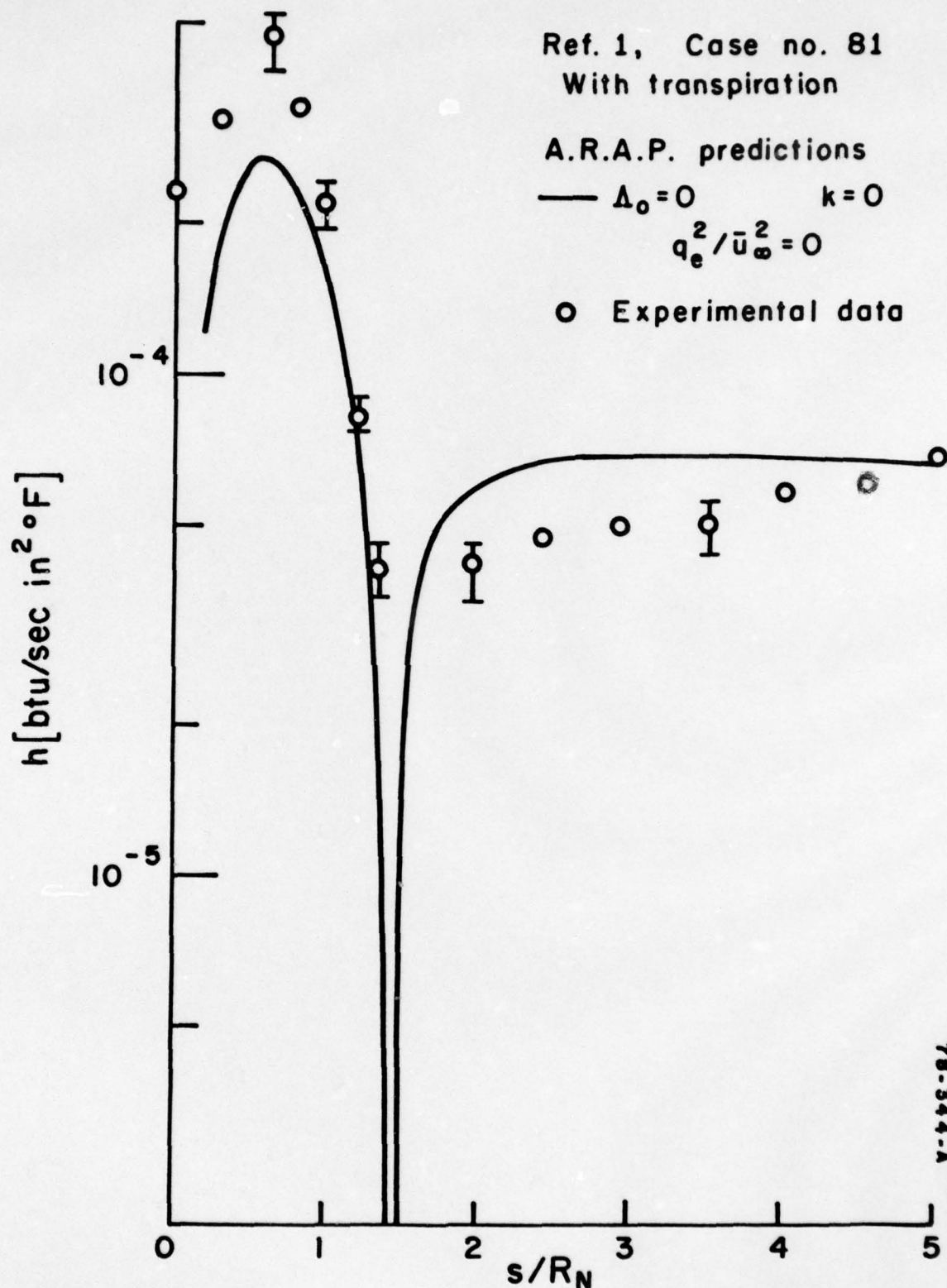


Figure 3.3. Calculated heat transfer coefficient for conditions of Case No. 81 (Ref. 1) for zero surface roughness and zero edge turbulence.  $Re_N = 2.95 \times 10^6$  with transpiration.

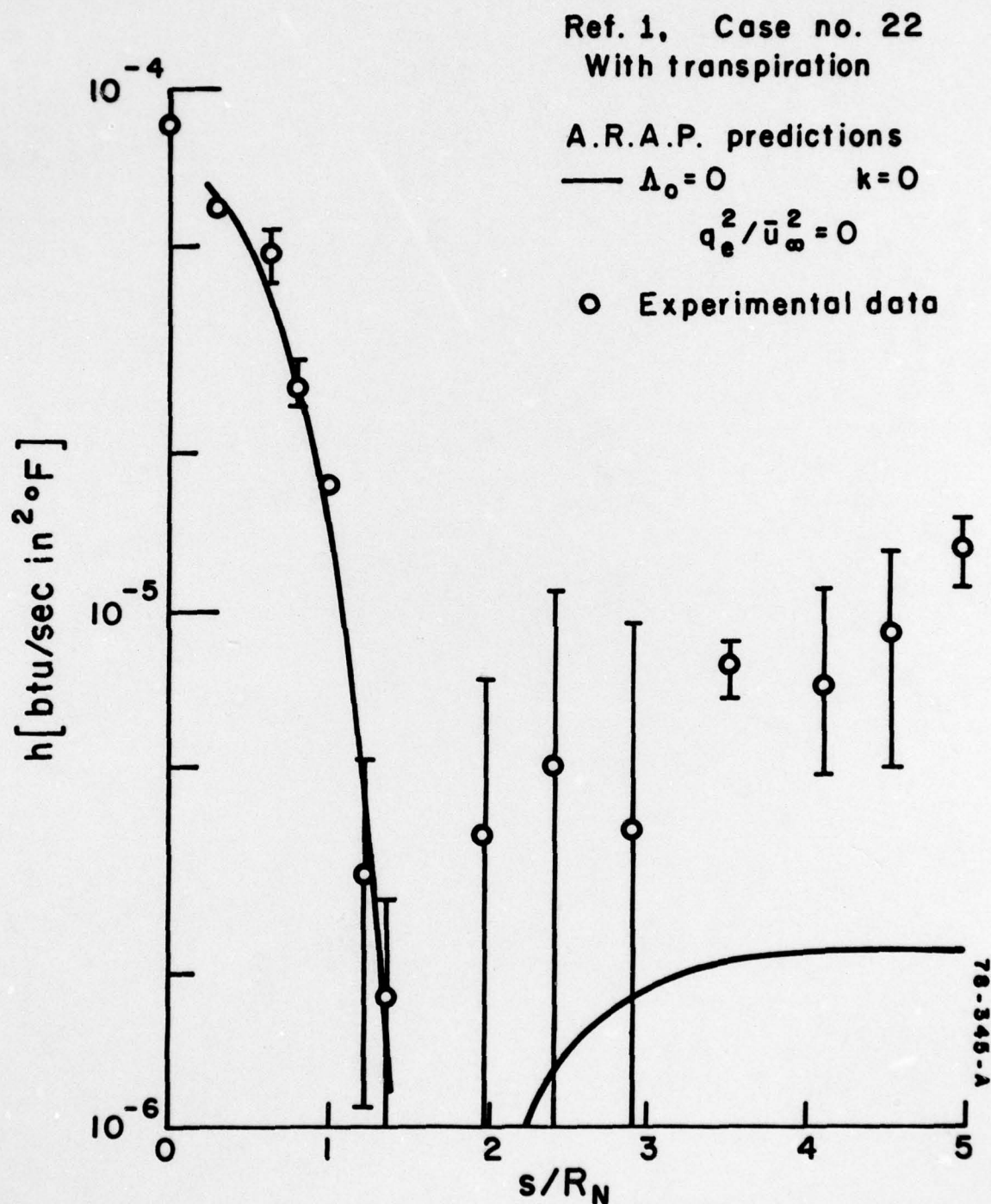


Figure 3.4. Calculated heat transfer coefficient for conditions of Case No. 22 (Ref. 1) for zero surface roughness and zero edge turbulence.  $Re_N = 6.33 \times 10^5$  with transpiration.



spot of turbulence we have assumed (Figs. 3.1 and 3.2). However, when the destabilizing effect of transpiration is included in the calculations, we find that the higher Reynolds number case exhibits early transition while the low Reynolds number case does not (Figs. 3.3 and 3.4). We note that the calculated heat transfers for the high Reynolds number case when there is zero roughness and zero free-stream turbulence are below those measured on the test sphere/cone. It is also clear from a detailed study of the computer output that the whole behavior of the flow in the stagnation point region is extremely sensitive to the turbulence that is introduced into the boundary layer in this region. Indeed, the occurrence of early transition will depend on a complex interaction of the Reynolds number, the free-stream turbulence level, the body roughness, the body temperature, the Mach number, and so forth.

Calculations with surface roughness. In Figs. 3.5 and 3.6 we show the effect of surface roughness for the case of high Reynolds number. For the case when there is no transpiration (Case 1), we show in Fig. 3.5 the effect of roughness through calculations having uniform roughness over the entire sphere/cone of the following levels:

$\Lambda_0 = 0$	$k = 0$
$\Lambda_0 = 3 \times 10^{-6}$ inches	$20 < k < 40$ microinches
$\Lambda_0 = 3 \times 10^{-5}$ inches	$200 < k < 400$ microinches
$\Lambda_0 = 3 \times 10^{-4}$ inches	$.002 < k < .004$ inches

It is clear from Fig. 3.5 that a surface roughness in the range from 20 to 40 microinches will not, according to these particular calculations, cause early transition at  $Re_N = 2.95 \times 10^6$  when there is no steady source of edge turbulence. However, if the roughness is increased to the order of from 200 to 400 microinches, early transition will occur. The level of heat transfer in the nose region is, by calculations, somewhat less than is observed experimentally for this level of



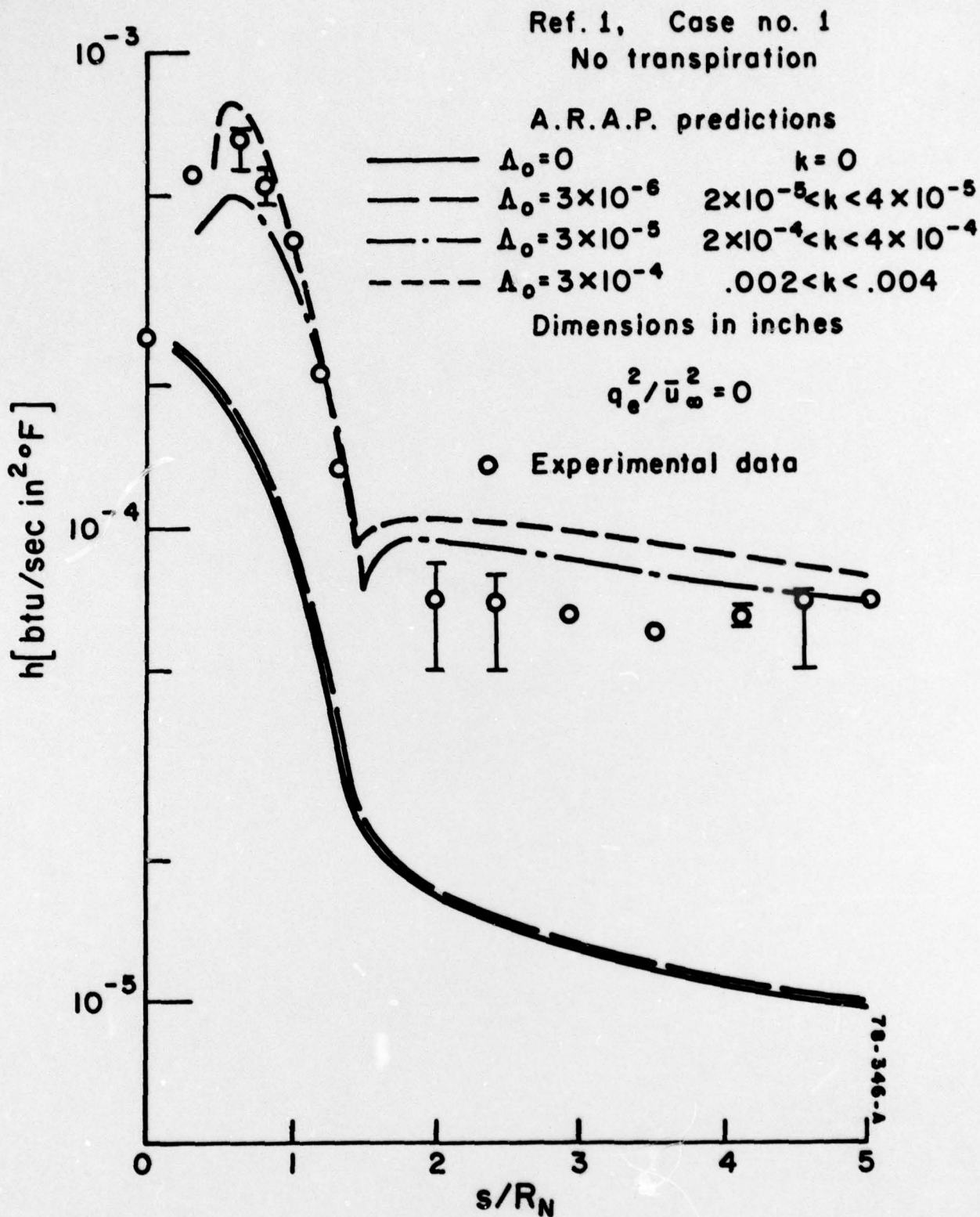


Figure 3.5. Parametric study of the effect of surface roughness on heat transfer with edge turbulence equal zero for Case No. 1 (Ref. 1).  $Re_N = 2.95 \times 10^6$  and no transpiration.

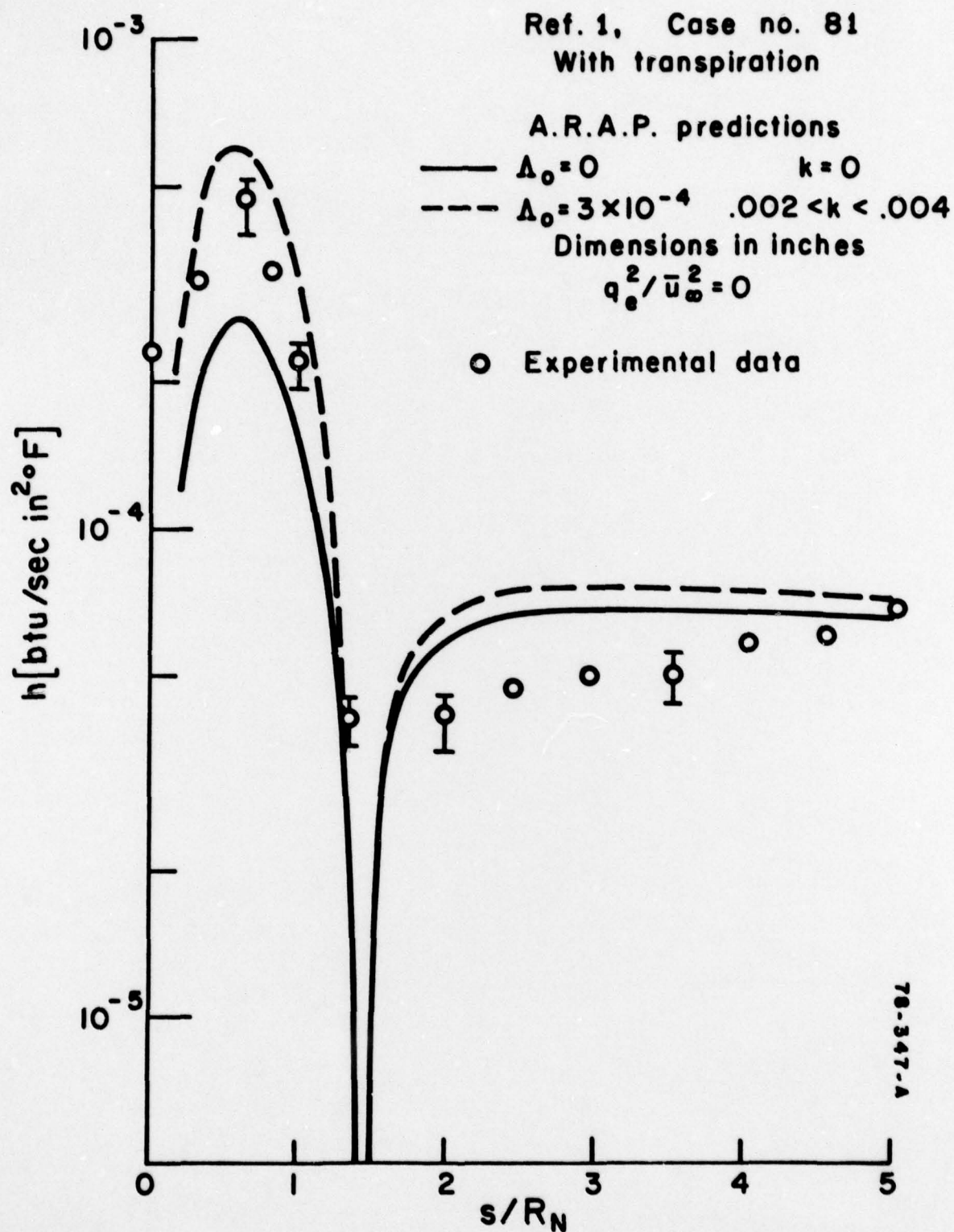


Figure 3.6. Effect of two surface roughnesses on heat transfer with edge turbulence equal zero for Case No. 81 (Ref. 1).  
 $Re_N = 2.95 \times 10^6$  with transpiration.

roughness. For roughness in the range from .002 to .004 inches, early transition occurs and the levels of heat transfer in the nose region are more nearly equal to the experimental values. For this larger roughness the calculated heat transfer to the conical region of the body is considerably higher than the experimental data. Although not shown in Fig. 3.5, calculations carried out for roughness of the order of .001 to .002 inches fell almost on top of the results for roughness of the order of .002 to .004 inches on the spherical portion of the body, and between the curves for  $200 < k < 400$  microinches and  $.002 < k < .004$  inches on the conical section of the body.

For the case when transpiration is considered at high Reynolds number (Case 81) we show calculations in Fig. 3.6 for

$$\Lambda_0 = 0$$

$$k = 0$$

$$\Lambda_0 = 3 \times 10^{-4} \text{ inches}$$

$$.002 < k < .004 \text{ inches}$$

Here again we see that roughness increases the turbulent heat transfer in the stagnation point region to values close to the experimental data on the spherical portion of the body as well as on the cone. As before, for levels of roughness that give heat transfer in agreement with experimental results on the spherical portion of the body, the heat transfer to the conical portion of the body is overpredicted. It appears that we are dealing with a problem where both the roughness level and boundary-layer edge turbulence level are needed to achieve a match to experimental data in both regions.

Calculations with roughness and free-stream turbulence. The final calculations we shall show to round out this preliminary study of the A.R.A.P. code are calculations where we have fixed the surface roughness at a value guessed at from the data just presented and varied the level of external turbulence impinging on the edge of the boundary layer. The same initial conditions as those used in the previous runs were used. This is not exactly correct, for if there were external turbulence, the turbulence



distribution at  $s/R_N = 0.1$  would not be a spike in the interior of the boundary layer with a uniform outer turbulence. However, in making these first calculations some parameters of the problem had to be held fixed.

The level of roughness chosen was  $.001 < k < .002$  inches. This roughness was placed only where there were porous surfaces on the model, that is for  $s/R_N < 3.24$ . The roughness was taken to be zero outside of this region. Two levels of boundary-layer-edge turbulence were investigated. They were  $q_e^2/\bar{u}_\infty^2 = 3 \times 10^{-6}$  and  $3 \times 10^{-7}$ . This turbulence was assumed to be isotropic in the sense that  $\bar{u}_e'^2/\bar{u}_\infty^2 = \bar{v}_e'^2/\bar{u}_\infty^2 = \bar{w}_e'^2/\bar{u}_\infty^2$ . The results are shown in Figs. 3.7 through 3.10.

For the high Reynolds number cases (Figs. 3.7 and 3.8), it is not worth plotting the curves for the separate values of  $q_e^2/\bar{u}_\infty^2$ , because the curves are not markedly different. In these cases the curves differ only in a small region close to the stagnation point and, without a proper initializing code, the differences in the results are probably not too meaningful. However, for the low Reynolds number cases (Figs. 3.9 and 3.10) the effect of free-stream turbulence is pronounced. Transition is occurring on the conical portion of the test body for these cases and the computed results are not in bad agreement with the experimental data. The rate at which transition is occurring does appear to be too fast. However, this may be due to the distribution of edge turbulence that has been assumed.

Before going on to make some general conclusions and recommendations for what might be future work, the effect of cutting off the roughness for the high Reynolds number cases at the end of the porous wall region,  $s/R_N = 3.24$  should be noted. The rapid drop in heat transfer at this point and the fact that computations give too high a heat transfer on the cone ahead of  $s/R_N = 3.24$ , would suggest that the roughness we have chosen is too high and the actual porous material roughness must be less than .001 to .002 inches. This deduction is strengthened when we



look at the peak heat transfer on the spherical portion of the body and note that with the combined effects of edge turbulence and roughness, we are slightly overestimating this heat transfer also.

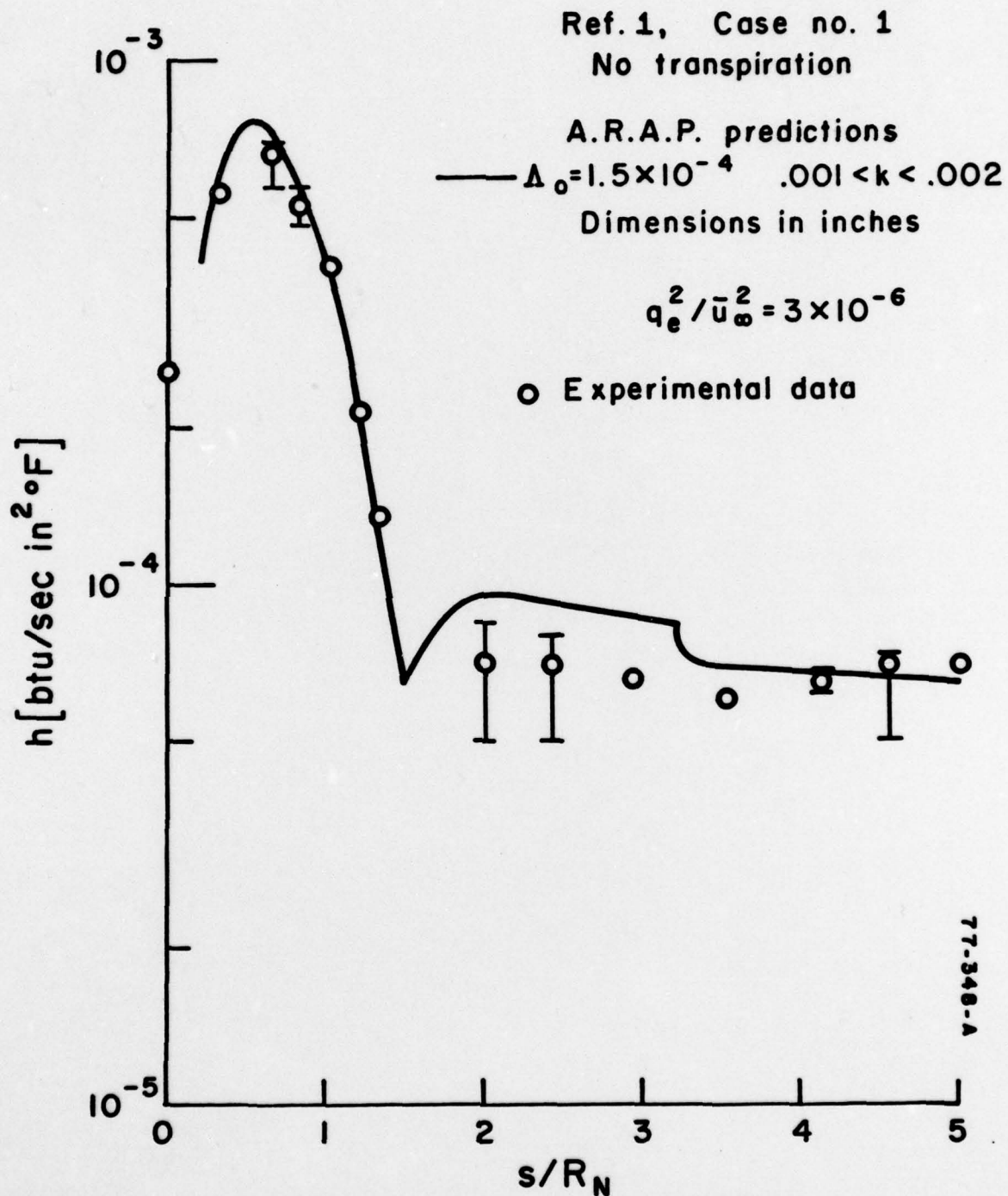


Figure 3.7. Calculated heat transfer coefficient for a particular choice of surface roughness and edge turbulence for Case No. 1 (Ref. 1).  $Re_N = 2.95 \times 10^6$  and no transpiration.

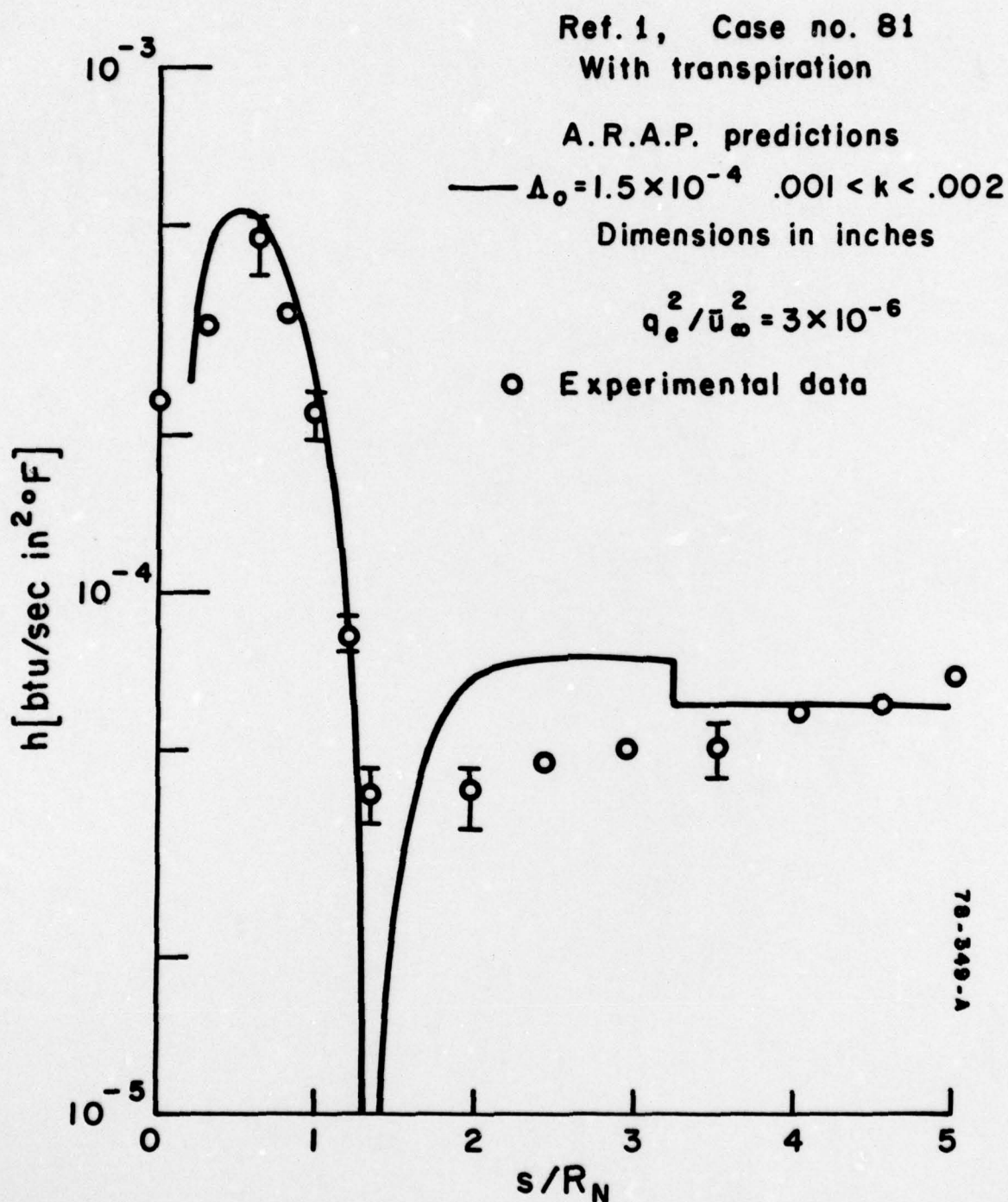


Figure 3.8. Calculated heat transfer coefficient for a particular choice of surface roughness and edge turbulence for Case No. 81 (Ref. 1).  $Re_N = 2.95 \times 10^6$  with transpiration.



Ref. 1, Case no. 2  
No transpiration

A.R.A.P. predictions  
 $\Delta_0 = 1.5 \times 10^{-4}$   $.001 < k < .002$   
Dimensions in inches

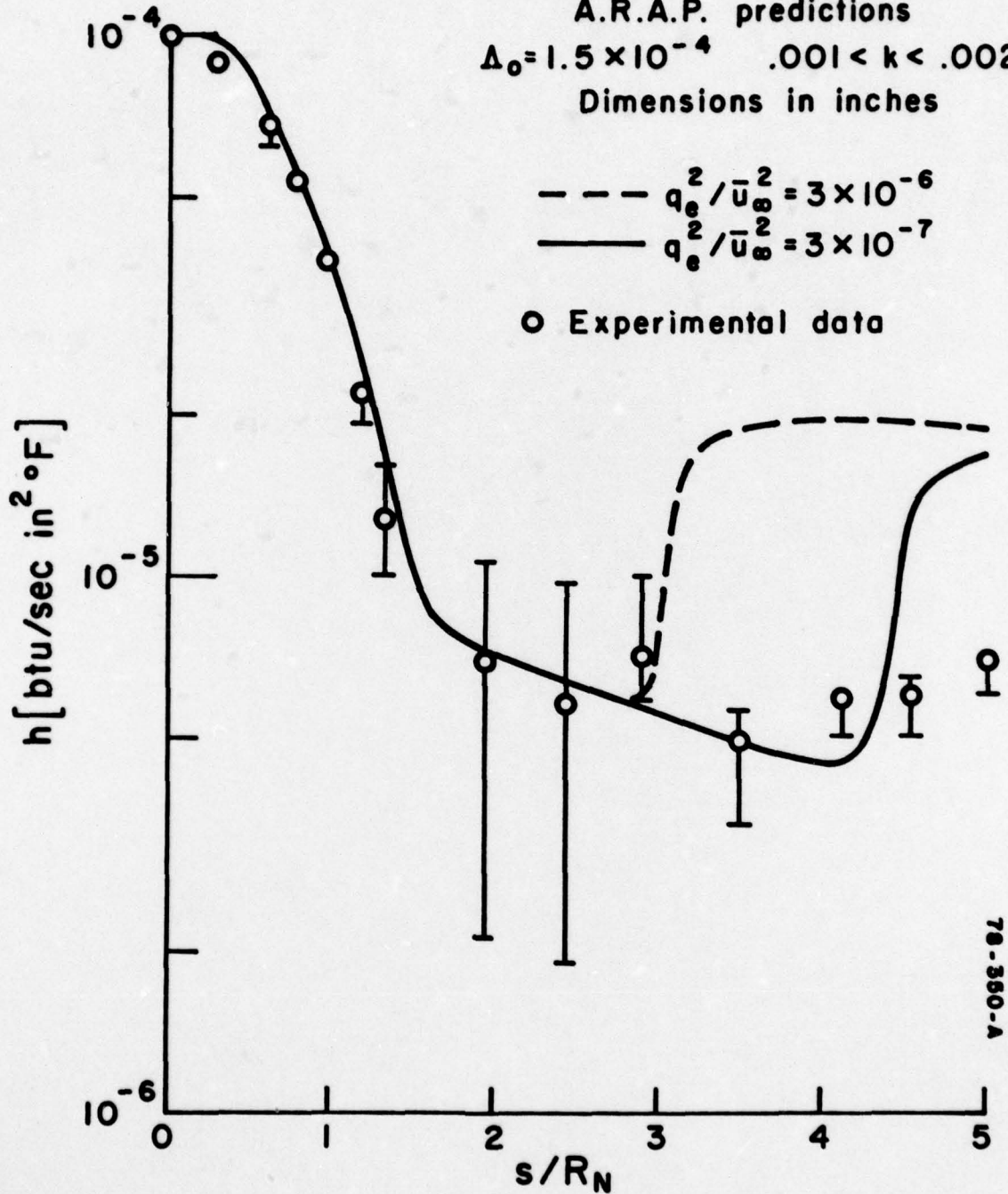


Figure 3.9. Calculated heat transfer coefficient for a particular choice of surface roughness and two choices of edge turbulence for Case No. 2 (Ref. 1).  $Re_N = 6.33 \times 10^5$  and no transpiration.

Ref. 1, Case no. 22  
With transpiration

A.R.A.P. predictions  
 $\Delta_0 = 1.5 \times 10^{-4}$   $.001 < k < .002$   
Dimensions in inches

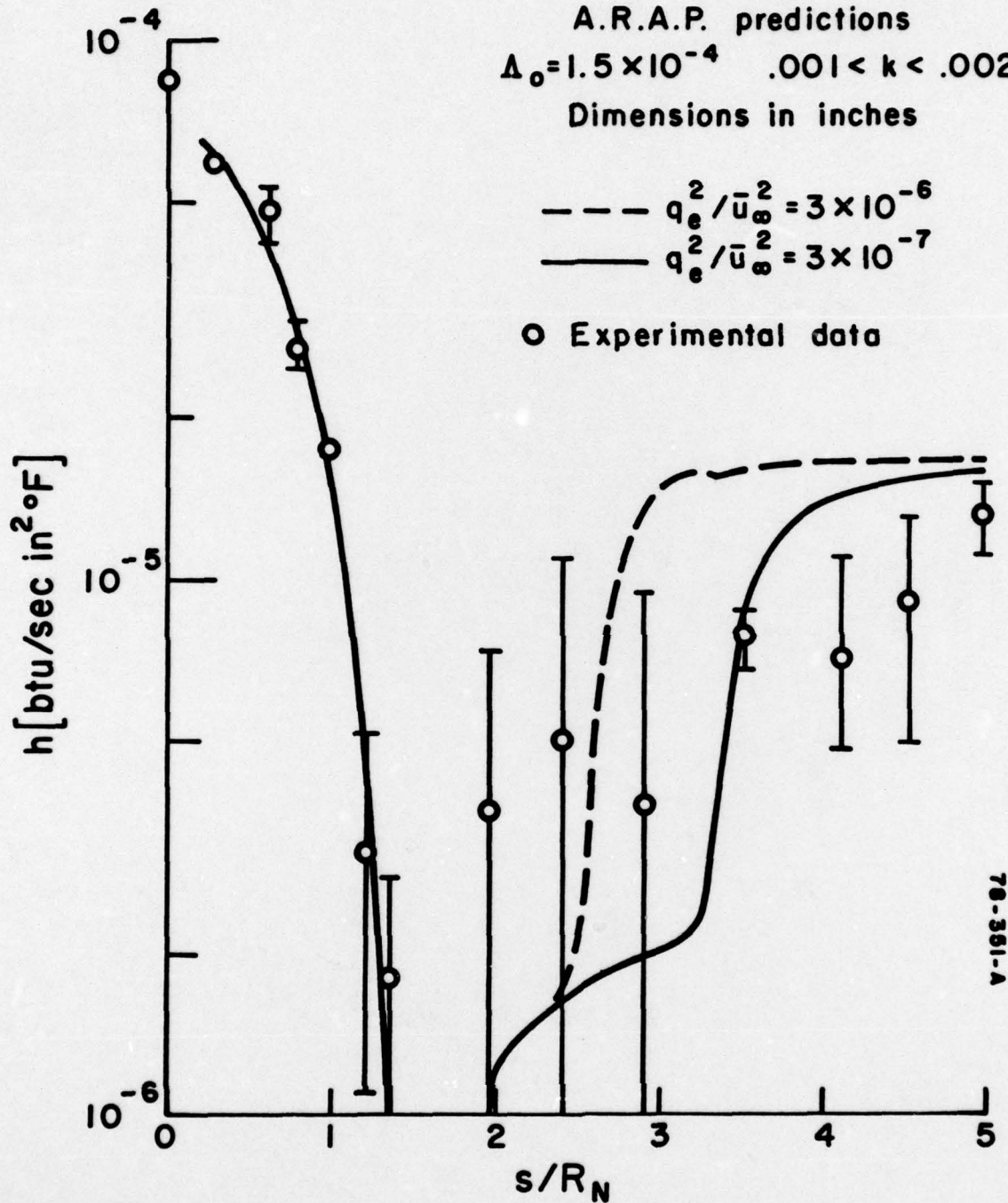


Figure 3.10. Calculated heat transfer coefficient for a particular choice of surface roughness and two choices of edge turbulence for Case No. 22 (Ref. 1).  $Re_N = 6.33 \times 10^5$  with transpiration.

#### 4. CONCLUSIONS AND RECOMMENDATIONS

We have given a very brief description of the results obtained in an initial study of the effects of surface roughness and boundary-layer-edge turbulence on the heat transfer to a blunt body with and without surface transpiration using the A.R.A.P. second-order-closure code. It seems that this code exhibits considerable promise for the calculation of boundary layer behavior on high-speed blunt bodies. Indeed, it would appear that, given a more complete parameter search, a choice of surface roughness and edge turbulence could be found that would give considerably better agreement between calculations and the experimental data we have so far examined. The values of roughness and turbulence that would do this appear to be very realistic.

It is recommended that a more extensive parametric study of the effects of surface roughness and edge turbulence than that carried out in demonstrating this code be carried forward using the code in its present form.

It is clear that an initializing code which will allow proper computation of stagnation point flows when the impinging flow contains turbulence fluctuations is desirable.

It is recommended that such an initializing code be developed forthwith.



## 5. REFERENCES

1. Feldhuhn, R.H.: Heat Transfer from a Turbulent Boundary Layer on a Porous Hemisphere. AIAA Preprint No. 76-119, January 1976.
2. Sullivan, R.D. and Varma, A.K.: ARB: A Program to Compute the Turbulent Boundary Layer on an Arbitrary Body of Revolution. A.R.A.P. Report No. 317, January 1978 (User's Manual).

DISTRIBUTION

Naval Sea Systems Command  
Washington, DC 20362  
Attn: Mr. L. Pasiuk/03512

Air Force Office of Scientific Research  
Bolling AFB, Bldg. 410  
Washington DC 20332  
Attn: B. Quinn

Arnold Engineering Development Center  
AFSC, USAF  
Arnold Air Force Station  
Tennessee 37389  
Attn: L. Potter

Naval Surface Weapons Center  
Silver Spring, Maryland 20910  
Attn: C. Lyons/K06  
R. Feldhuhn/K82  
J. Goeller/K82  
R. Phinney/U14  
C. A. Fisher/K80  
S. Hastings/K80  
R. Schlie/K81  
Librarian (3 copies)

Office of Naval Research  
800 N. Quincy  
Arlington VA 22217  
Attn: M. Cooper

General Electric Corp.  
3198 Chestnut Street  
Philadelphia PA 19101  
Attn: T. Shaw  
R. Neff  
D. Nestler

Jet Propulsion Laboratory  
4800 Oak Grove Drive  
Pasadena, CA 91103  
Attn: L. Mack

SAMSO  
P.O. Box 92960  
Los Angeles Air Force Station  
Los Angeles, CA 90009  
Attn: LTCOL J. McCormack/RSSE  
CAPT R. Chambers/RSSE

Institute for Defense Analysis  
Science and Technology Division  
400 Army-Navy Drive  
Arlington, VA 22202  
Attn: P. Liepman

Aerotherm/Acurex Corporation  
485 Clyde Avenue  
Mountain View, CA 94040  
Attn: R. Rindal

Avco Systems Division  
201 Lowell Street  
Wilmington Massachusetts 01852  
Attn: A. Pallone

McDonnell-Douglas Corporation  
5301 Bolsa Avenue  
Huntington Beach, CA 92647  
Attn: J. S. Murphy

Aeronutronic Ford  
Space and Reentry Systems  
Ford Road  
Newport Beach, CA 92663  
Attn: A. Demetriades

Physical Sciences, Inc.  
18 Lakeside Office Park  
Wakefield, Massachusetts 01880  
Attn: M. Finson

Department of Aerospace Engineering  
University of Southern California  
Los Angeles, CA 90007  
Attn: J. Laufer  
E. Van Driest

SAMSO/MNNR  
Norton AFB, CA 92409  
Attn: LTCOL J. Brown

Air Force Wright Aeronautical Lab  
Wright-Patterson AFB  
Ohio 45433  
Attn: W. Hankey/AFFDL  
B. Kessler/AFML

Enclosure (1)

DISTRIBUTION (Continued)

Aerospace Corproation  
P.O. Box 92957  
Los Angeles, CA 90009  
Attn: R. Mortenson  
T. Taylor

Navy Department  
Strategic Systems Project Office  
Washington, DC 20360  
Attn: SP-272

Lockheed Missiles and Space Co.  
1111 Lockheed Way  
Sunnyvale, CA 94088  
Attn: C. Lee  
P.J. Schneider

TRW  
1 Space Park  
Redondo Beach, CA 90278  
Attn: Technical Library

PDA  
1740 Garry Avenue  
Santa Ana, CA 92705  
Attn: M. Sherman

SAI  
1200 Prospect St.  
LaJolla, CA 92037  
Attn: T. Martellucci  
K. Kratsch

Polytechnic Institute of New York  
Department of Aerospace Engineering  
and Applied Mechanics  
Route 110  
Farmingdale, NY 11735  
Attn: R. Cresci

Prof. Paul Libby  
University of California San Diego  
La Jolla, CA 92037

NASA Langley Research Center  
Hampton, VA 23665  
Attn: J. Harris

The RAND Corporation  
1700 Main Street  
Santa Monica, CA 90406  
Attn: C. Gazley

NASA Ames Research Center  
Moffett Field, CA 94035  
Attn: M. Rubesin  
C. Horstmann  
G. Kaatarri  
H. Larson

Princeton University  
Forrestal Research Center  
Gas Dynamics Laboratory  
Princeton, NJ 08540

Stanford University  
Department of Mechanical Engineering  
Stanford, CA 94305  
Attn: R. J. Moffatt

Virginia Polytechnic Institute and  
State University  
Department of Aerospace Engineering  
Blacksburg, VA 24061  
Attn: Dr. G. R. Inger

Dr. Eli Reshotko  
Case Western Reserve University  
Glennan Building  
University Circle  
Cleveland, Ohio 44106

DCW Industries  
4367 Troost Avenue  
Studio City, CA 91604